cogent engineering

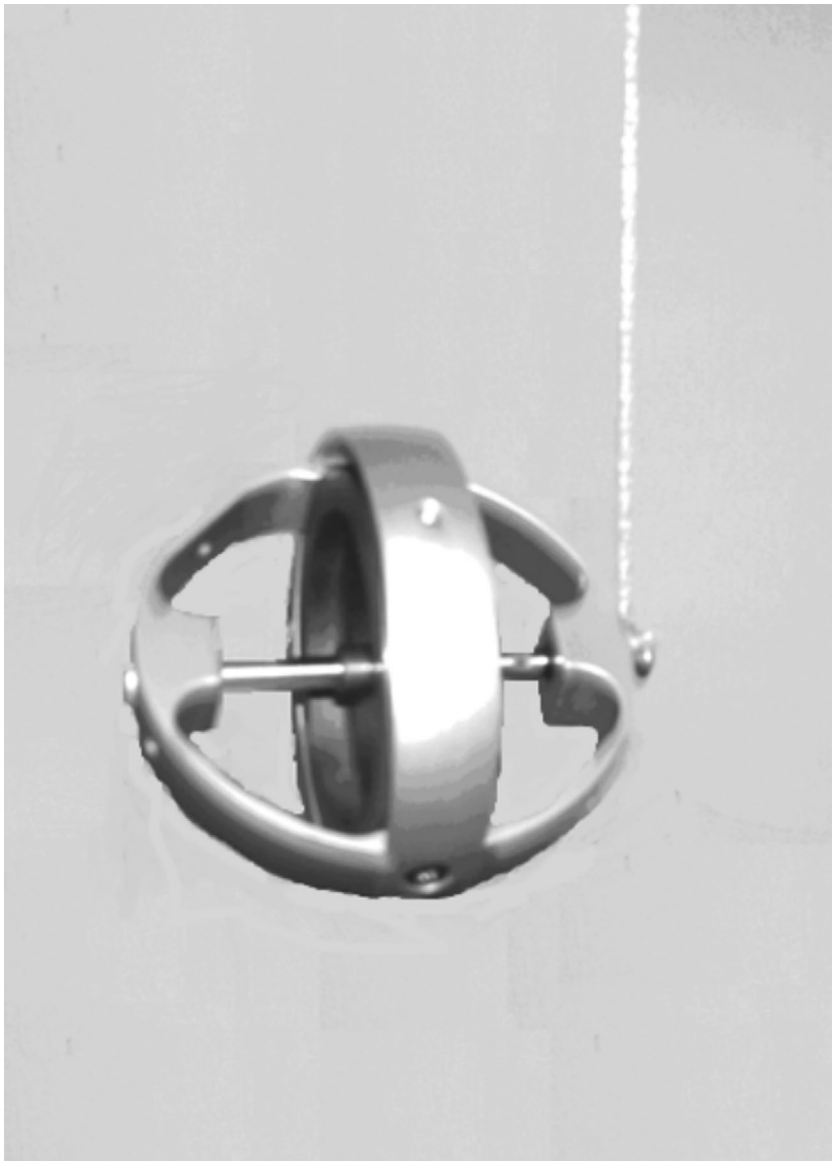

MECHANICAL ENGINEERING | RESEARCH ARTICLE

A mathematical model for motions of gyroscope suspended from flexible cord

Ryspek Usubamatov

Cogent Engineering (2016), 3: 1245901

Usubamatov, *Cogent Engineering* (2016), 3: 1245901
http://dx.doi.org/10.1080/23311916.2016.1245901

cogent engineering

MECHANICAL ENGINEERING | RESEARCH ARTICLE

A mathematical model for motions of gyroscope suspended from flexible cord

Ryspek Usubamatov[1]*

Received: 24 June 2016
Accepted: 04 October 2016
First Published: 11 October 2016

*Corresponding author: Ryspek Usubamatov, Mechanical, Manufacturing and Industrial Engineering, International University of Kyrgyzstan, 255 Chui Avenue, Bishkek, Kyrgyz Republic
E-mail: ryspek0701@yahoo.com

Reviewing editor:
Duc Pham, University of Birmingham, UK

Additional information is available at the end of the article

Abstract: Gyroscope devices are primary units for navigation and control systems in aviation and space engineering. The main property of the gyroscope is maintaining the axis of a spinning rotor, based on the principles of the angular momentum of the spinning rotor. However, the nature of the gyroscope's acting forces and motions is more complex. The torque applied to the gyroscope generates the internal resistance and precession torques based on acting simultaneously and interdependently, namely, centrifugal, common inertial and Coriolis forces generated by the mass elements of the spinning rotor as well as changes in angular momentum. This system of internal torques based on new fundamental principles of the gyroscope theory that enabled deriving the mathematical model for the motions of a gyroscope suspended from the flexible cord, which was a most unsolvable problem. The test results of the gyroscope motions well validated the new analytical approach.

Subjects: Engineering Education; Mechanical Engineering; Mechanical Engineering Design

Keywords: gyroscope theory; property; test, torque

1. Introduction

In 1765, L. Euler first laid the mathematical foundations for the gyroscope theory in his work on the dynamics of rigid bodies. Other brilliant scientists had investigated, developed and added new interpretations for gyroscope effects, which are displayed in the rotor's persistence of maintaining its plane of rotation. The applied theory of gyroscopes, i.e. the theory of devices and gyroscopic

Ryspek Usubamatov

ABOUT THE AUTHOR

Prof Dr Eng. Ryspek Usubamatov graduated from Bauman Moscow State Technical University in 1966. He obtained Professional Engineer Diploma in Mechanical, Manufacturing and Industrial Engineering, PhD in Automation of Manufacturing Processes in 1972 and Doctor of Technical Sciences in 1993. He worked as engineer-designer of machine tools at engineering company and lecturer and researcher in a number of universities in Central Asia and Malaysia. He has supervised around 100 Professional Engineer students, 15 Master of science, 7 Doctoral and Post Doctoral students in his areas of interest. His key research activities are Productivity Theory for Industrial Engineering and Gyroscope Theory that represented by 7 books, 30 brochures and more than 300 manuscripts and 60 patents of inventions in engineering.

PUBLIC INTEREST STATEMENT

The simplest gyroscopes are known as the top toys that were invented in many different civilizations of mankind thousands of years ago and still attract attention by their astonishing capabilities and amaze by their unusual properties. The main property of the gyroscope is maintaining the axis of a spinning rotor. This property of a gyroscope is used unit for navigation and control in aviation, space, ships and other industries. However, the gyroscope demonstrates several effects which the science could not provide a good explanation or a mathematical description for the long time. Finally, the recent investigations enable the describing the physical principles of the acting forcers in a gyroscope and expressed by the mathematical models. This mathematical model tested and validated practically on the gyroscope suspended from flexible cord that was most unsolvable problem. New principles enable the solving all gyroscope properties, produce perfect the gyroscopes and monitoring their work.

systems, emerged mainly in the twentieth century (Cordeiro, 2015; Greenhill, 2015; Neil, 2014; Scarborough, 2014). Gyroscopic effects and properties are relayed in many engineering calculations for rotating parts that enable the function of numerous gyroscope devices in aviation and space, on ships and in other industries (Jonsson, 2007; Weinberg, 2011). All fundamental textbooks of classical mechanics contain chapters that represent the gyroscope theory (Aardema, 2005; Gregory, 2006). However, the studies of physical effects that regard the behavior of gyroscopes still remain inadequately explained (Liang & Lee, 2013).

There are many publications and a great number of mathematical solutions that describe spinning rotor properties (Crassidis & Markley, 2016; Zhang, Ren & Li, 2012). All publications contain numerous assumptions and simplifications and explain gyroscope effects in terms of the conservation of kinetic energy, as well as by the action of the internal moments (Doupe & Swenson, 2016; Stevenson & Schaub, 2012). Some researchers have intuitively pointed to the action on the gyroscope of other inertial forces that also take part in the manifestation of gyroscope effects (Braun, Putnam, Steinfeldt, Grant, & Barton, 2013). This is, therefore, the deficiency of all previous studies of gyroscope properties that are based only on one principle of the change in the angular momentum. Due to this, all mathematical models for the gyroscope effects do not match practical applications for gyroscopic devices. Experts in the area of the gyroscope theories confirmed this statement. This is why the gyroscope problems still attract many researchers to seek and discover new properties for these devices (Inampudi & Gordeuk, 2016).

The nature of gyroscope effects is more complex than those represented in the known theories. Researchers did not pay attention to the action of the inertial forces generated by the mass elements of the spinning rotor, and they considered the action of the gyroscope center-mass only. Recent investigations of the physical principles of gyroscope motions demonstrate that the four classical inertial forces generated by the mass elements are acting upon a spinning rotor and resulting in all gyroscope motions. Research shows that centrifugal, common inertial and Coriolis forces produced by the mass elements as well as the change in the angular momentum of the spinning rotor are the basis of all gyroscopic effects and properties. New studies demonstrate that the external torque applied to the gyroscope generates several internal torques based on the action of the forces mentioned. In turn, the centrifugal and Coriolis forces generate a resistance torque that counteracts the inclination of the rotor's location. Other than that, common inertial forces and change in the angular momentum of a spinning rotor generate a precession torque. All torques are interrelated, occur simultaneously and can be combined to depend on the action of the external torques applied to the gyroscope. These gyroscope internal torques are real active physical components, and the well-known change in the angular momentum, that is, the non-primary acting component, which does not play the first role in gyroscope properties. The results of new studies make it clear why the gyroscope theory is far from perfection (Usubamatov, 2014, 2015, 2016).

New mathematical model for gyroscope motions demonstrates the interdependent action of eight internal torques around two axes. Moreover, this model manifests new gyroscope properties, interprets known unexplainable ones and is validated by tests conducted on the precision gyroscope. These new fundamental principles for gyroscope theory represent new challenges for future studies of gyroscopic devices.

This proposed paper presents a mathematical model for the motions of a gyroscope with one side suspended from the flexible cord under the action of the load and internal torques. The load torque is represented by the action of the gyroscope weight and internal gyroscope torques by resistance and precession torques. Furthermore, the new mathematical model describes the gyroscope motions accurately and its results match practical tests. The model for the gyroscope motions was tested on the Super Precision Gyroscope (Brightfusion Ltd, Abbeymead, UK) with measurements of the times of motions.

2. Methodology

New studies into the physical principles of gyroscopic motions have presented mathematical models for the so-called gyroscopic resistance and precession torques, whose equations are shown in Table 1. The resistance torque is generated by the action of the centrifugal and Coriolis forces of the gyroscope's mass elements. The action of the common inertial forces of mass elements and the well-known change in the angular momentum of the spinning rotor produce the precession torques. These resistance and precession torques are interrelated, act at the same time and are strictly perpendicular to each other around their axes.

The equations of acting torques (Table 1) contain the following symbols: J is the rotor's mass moment of inertia around its own axis; ω_i is the angular velocity of the precession of a spinning rotor around axis i and ω is the angular velocity of a spinning rotor. For clarity in the following analyses of the actions of several torques and motions around axes, all components of the equations are marked by subscript signs that indicate the axis of action. For example, T_{rx} is the resistance torque acting around axis ox, ω_y is the angular velocity of precession around axis oy, etc.

The equations of the load and internal torques acting on the gyroscope are used to formulate the mathematical model for the motions around two axes of a gyroscope suspended from the flexible cord. This example represents the most unsolvable problem in the gyroscope theory. Furthermore, the analytical model for the motions is considered in the Super Precision Gyroscope by Brightfusion Ltd. Figure 1(a) demonstrates the running gyroscope suspended from the flexible cord. The gyroscope was assembled with the ability to freely rotate around axes ox and oy of the cord. A detailed picture of the gyroscope's geometrical and computed technical parameters is shown in Figure 1(b) and in Table 2, respectively.

Tables 2 and 3 contain the following symbols: J_x and J_y are the mass moment of the gyroscope's inertia around axes ox and oy, respectively; l is the overhang of the centre of gravity of the gyroscope from the support o, while m is the mass of the gyroscope components; R is the radius of the rotor's disc.

The mathematical model of motions for the gyroscope suspended from the flexible cord is formulated for the common case when its axle is inclined at the angle γ. Besides that, the analysis of the torques and motions acting in the gyroscope is conducted on the basis of several rules and regulations. The external load torque T that is produced by the gyroscope weight W generates the following internal resistance and precession torques, which are interrelated and act at the same time around axes ox and oy.

(a) The resistance torques are generated by the action of centrifugal $T_{ct\cdot x}$ and Coriolis forces $T_{cr\cdot x}$ of mass elements acting around axis ox.

(b) The precession torques are generated by common inertial forces $T_{in\cdot x}$ of mass elements and the rate change in the angular momentum of spinning rotor $T_{am\cdot x}$ acting around axis oy.

Table 1. Internal torques acting on a gyroscope

Type of torque generated by	Equation (N.m)
Centrifugal forces (T_{ct})	$T_{ct} = T_{in} = 2\left(\frac{\pi}{3}\right)^2 J\omega\omega_i$
Inertial forces (T_{in})	
Coriolis forces (T_{cr})	$T_{cr} = (8/9)J\omega\omega_i$
Change in angular momentum (T_{am})	$T_{am} = J\omega\omega_i$
Resistance torque ($T_r = T_{ct} + T_{cr}$)	$T_r = \left[2\left(\frac{\pi}{3}\right)^2 + \frac{8}{9}\right] J\omega\omega_i$
Precession torque ($T_p = T_{in} + T_{am}$)	$T_p = \left[2\left(\frac{\pi}{3}\right)^2 + 1\right] J\omega\omega_i$

Figure 1. The gyroscope suspended from the flexible cord.

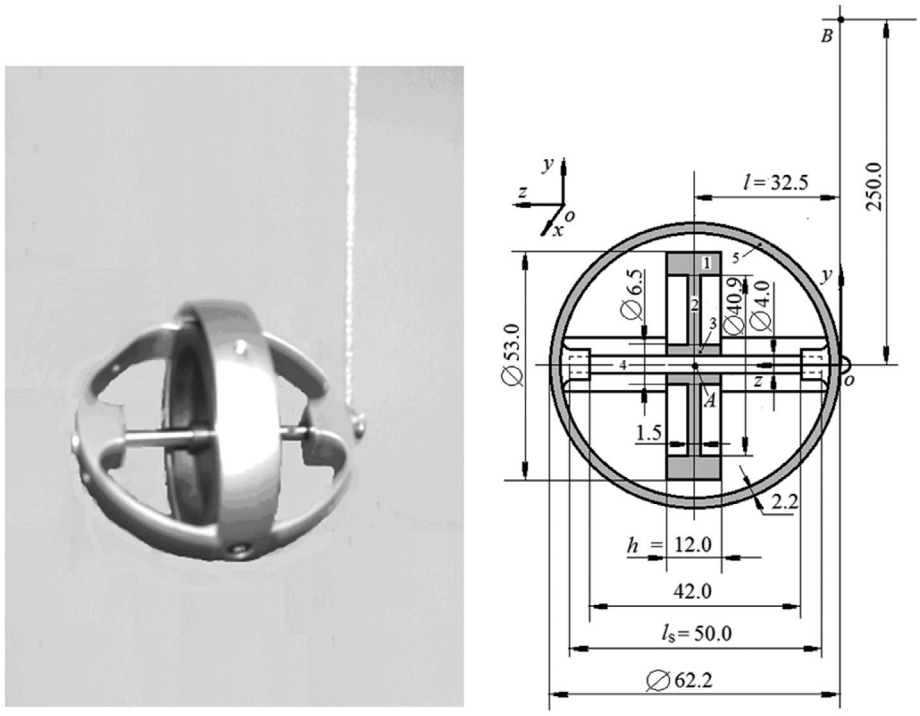

(c) The precession torques $T_{in\cdot x}$ and $T_{am\cdot x}$, in turn, generate the precession torques of inertial forces $T_{in\cdot y}$ of mass elements and the rate change in angular momentum $T_{am\cdot y}$ acting around axis *ox*, and the resistance torques of centrifugal forces $T_{ct\cdot y}$ and Coriolis forces $T_{cr\cdot y}$ of mass elements acting around axis *oy*.

(d) The rotating gyroscope centre-mass around axis *oy* generates the centrifugal force that produces the torque $T_{ct\cdot my}$ acting around axis *ox*.

The action of the external and internal torques is represented graphically in Figure 2.

Table 2. Technical data of the test stand with Super Precision Gyroscope, "Brightfusion LTD"

Weight	Total rotating components		0.1159 kg
	Frame with bearings and screws		0.0294 kg
	Gyroscope (*W*)		0.1453 kg
	Total gyroscope with screw (*W*)		0.146 kg
Mass moment of inertia (*J*, kgm^2)	Around axis *oz*	Rotating components	0.5726674×10^{-4}
	Around axis *ox* and *oy*	Total	1.9974649×10^{-4}

Table 3. Mass moments of inertia for the gyroscope components

Title	Equation
Gyroscope mass moment of inertia around axis *ox* and *oy*	$J_x = J_y = (mR^2/4) + ml^2$
Rotor's mass moment of inertia around axis *ox* and *oy*	$J_x = J_y = (mR^2/4)$
Rotor's mass moment of inertia around axis *oz*	$J = (mR^2/2)$

Figure 2. The torques and motions acting on the gyroscope suspended from the flexible cord.

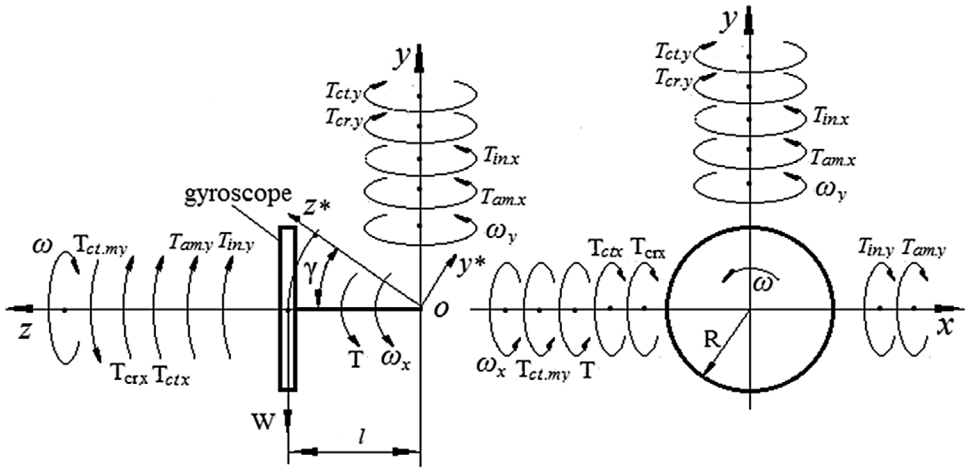

Figure 3. Vectors of gyroscope internal torques acting around two axes.

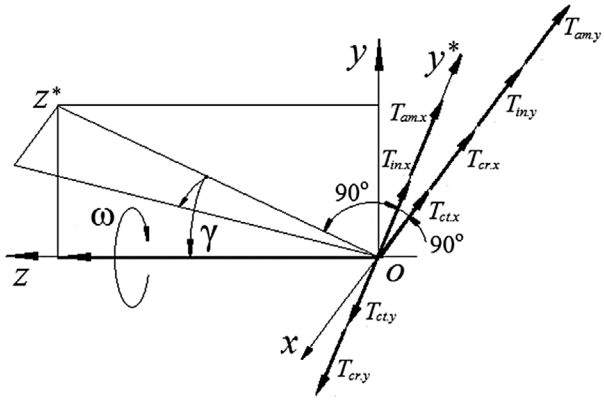

Figure 3 depicts the location of the vectors of the internal torques at the system of coordinate Σ*oxoz* for the Figure 2. Where *oz** is the axis of the spinning rotor, $T_{pi} = T_{in\text{-}i} + T_{am\text{-}i}$ and $T_{ri} = T_{ct\text{-}i} + T_{cr\text{-}i}$ is the vectors of precession and resistance torques acting around axis *ox* and *oy**, respectively, γ is the angle of the inclination of the spin axis. In space, the vectors of internal torques are always perpendicular between each other and to the axis of the spinning rotor *oz**.

All internal torques represented the internal kinetic energies of the spinning rotor generated by the external torque. The internal kinetic energy of each axis originated only by resistance and precession torques that are equal to the internal kinetic energy of the other axis. This statement is proved by the equation that obtained from Figure 3. The resistance torques of one axis are combined with precession torques of the other axis. The actions of these internal torques can be contradicted in a gyroscope that depends on the types of the external loads. However, each axis contains resistance and precession torques that originated in different axes. These combinations of internal torques can change the magnitudes of the angular velocities of the gyroscope around axes, but kinetic energies of each axis in absolute values remain constant.

The gyroscope properties, obtained through practical tests, are used for the mathematical models of the gyroscope motions (Usubamatov, 2014, 2016). The tests of the gyroscope were conducted in conditions of the action of all torques on the gyroscope's support. The objective of the tests is to validate the mathematical model for the action of the external and internal torques and motions of the gyroscope. Thus, the test results recorded the time of the gyroscope rotating around axes *ox* and *oy*.

The technical data of the gyroscope stand (Table 2 and Figures 1 and 2) enable the following information to be used for mathematical modelling of the gyroscope motions.

The action of load torque *T* around axis *ox* is represented by the following equation:

$$T = Wgl\cos\gamma \tag{1}$$

where *g* is the gravity acceleration, γ is the angle of the gyroscope's axle inclination and other components are as specified above.

The weight of the gyroscope acts positively in a counter-clockwise direction. The other torques acting in the gyroscope are represented by the several components whose directions are opposite and aside from the action of the load torque. Furthermore, the load torque *T* produces the several resistance and precession torques acting around axes *ox* and *oy*. The tests for the motion of the gyroscope demonstrated that its rotation around axis *oy* was carried out with a high angular velocity, faster than around axis *ox*. At first sight, this gyroscope property contradicts the rules of classical mechanics. However, analyses of the acting torques and motions in the gyroscope enable this property to be explained by the new mathematical model.

The mathematical model for the motions of the gyroscope suspended from flexible cord around axes *ox* and *oy* is represented by Euler's differential equations as follows:

$$\begin{aligned} J_x\frac{d\omega_x}{dt} &= T\cos\gamma + T_{ct\cdot my} - T_{ct\cdot x} - T_{cr\cdot x} - T_{in\cdot y}\cos\gamma - T_{am\cdot y}\cos\gamma \\ J_y\frac{d\omega_y}{dt} &= T_{in\cdot x}\cos\gamma + T_{am\cdot x}\cos\gamma - T_{ct\cdot y}\cos\gamma - T_{cr\cdot y}\cos\gamma \end{aligned} \tag{2}$$

where ω_x and ω_y are the angular velocity of the gyroscope around axes ox and oy, respectively; $T_{ct\cdot x}$, $T_{ct\cdot y}$, $T_{cr\cdot x}$, $T_{cr\cdot y}$, $T_{in\cdot x}$, $T_{in\cdot y}$, $T_{am\cdot x}$ and $T_{am\cdot y}$ are internal torques generated by the centrifugal, Coriolis, common inertial forces and by the change in the angular momentum, and acting around axes ox and oy, respectively, $T_{ct\cdot my}$ is the torque generated by the centrifugal force of the rotating gyroscope centre-mass around axis oy that acts around axis ox (Table 1 and Figure 2).

The centrifugal force of the rotating gyroscope centre-mass around axis *oy* produces the torque acting around axis *ox* and is defined by the following equation:

$$T_{ct\cdot my} = F_{ct\cdot my}\times l\sin\gamma = Wl\cos\gamma\,\omega_y^2\times l\sin\gamma = Wl^2\cos\gamma\sin\gamma\,\omega_y^2 \tag{3}$$

where $F_{ct\cdot my} = Wl\cos\gamma\,\omega_y{}^2$ is the centrifugal force of the gyroscope centre-mass rotating around axis *oy* and other components are as specified above.

Substituting the defined equations of the internal torques of the gyroscope (Table 1) as well as Equations (1) and (3) into Equation (2) enables the representing of the following system of differential equations:

$$\begin{aligned} J_x\frac{d\omega_x}{dt} &= Wgl\cos\gamma + Wl^2\cos\gamma\sin\gamma\omega_y^2 - 2\left(\frac{\pi}{3}\right)^2 J\omega\omega_x - \frac{8}{9}J\omega\omega_x - 2\left(\frac{\pi}{3}\right)^2 J\omega\omega_y\cos\gamma - J\omega\omega_y\cos\gamma \\ J_y\frac{d\omega_y}{dt} &= 2\left(\frac{\pi}{3}\right)^2 J\omega\omega_x\cos\gamma J\omega\omega_x\cos\gamma - 2\left(\frac{\pi}{3}\right)^2 - J\omega\omega_y - \frac{8}{9}J\omega\omega_y\cos\gamma \end{aligned} \tag{4}$$

where all the components are as specified above.

The two equations (Equation (4)) represent the system with two variables and demonstrate the following properties. The load torque *T* acting around axis *ox* produces two precession torques: $T_{in\cdot x}$ generated by the common inertial forces of mass elements, and torques $T_{am\cdot x}$ generated by the

change in the angular momentum. These torques are acting around axis *oy* while the actions of load *T* and precession torques $T_{in{\cdot}x}$ and $T_{am{\cdot}x}$ around the axes do not coincide. In turn, the precession torques $T_{in{\cdot}x}$ and $T_{am{\cdot}x}$ that act around axis *oy* demonstrate the same property of the action by the torques $T_{in{\cdot}y}$ and $T_{am{\cdot}y}$ but around axis *ox* (Figure 2). The rotating gyroscope centre-mass around axis *oy* produces the centrifugal force that acts as the torque $T_{ct{\cdot}my}$ around axis *ox* in the same direction as load torque *T*.

These interrelations of the torques acting around the two axes represent the gyroscope properties that cannot be formulated by a single mathematical equation. Hence, it can be stated that Equation (4) represents one specific equation with two components and two variables, which are the precession angular velocities around axes *ox* and *oy*. These gyroscope angular velocities are produced by the action of one load torque *T* and nine internal torques. The second equation of Equation (4) is part of one system that cannot be considered separately. This equation does not contain the load torque *T* and cannot be used for solving variables. Besides that, the solution of Equation (4) is possible by a third equation that can be formulated on the basis of the gyroscope's internal kinetic energy.

The system of Equation (4) contains eight internal torques generated by rotating mass elements, which are the internal kinetic energy of the spinning rotor (Table 1) and represent one system. The internal torque $T_{ct{\cdot}my}$ generated by the centrifugal force of rotating gyroscope centre-mass around axis *oy* has a different nature. This torque is separated from the system of torques generated by spinning mass elements of the gyroscope rotor. Hence, the equality of internal kinetic energies of the system of torques acting around axes *ox* and *oy* (Figure 2) formulated the following equation:

$$-T_{ct{\cdot}x} - T_{cr{\cdot}x} - T_{in{\cdot}y}\cos\gamma - T_{am{\cdot}y}\cos\gamma = T_{in{\cdot}x}\cos\gamma + T_{am{\cdot}x}\cos\gamma - T_{ct{\cdot}y}\cos\gamma - T_{cr{\cdot}y}\cos\gamma \tag{5}$$

where the left equation contains the torques $T_{ct{\cdot}x}$, $T_{cr{\cdot}x}$, while $T_{in{\cdot}y}$, and $T_{am{\cdot}y}$ are acting around axis *ox* and represent the resistance torques with the minus sign (−). Other than that, the right equation contains the precession torques $T_{in{\cdot}x}$ and $T_{am{\cdot}x}$ that are positive acting and the resistance torques $T_{ct{\cdot}y}$, and $T_{cr{\cdot}y}$ that are negative acting around axis *oy*. Other components are as specified above.

Equation (4) enables the dependency between the angular velocities of gyroscope precessions around axes *ox* and *oy* to be defined. Substituting the expressions of torques (Table 1) into Equation (5) and transforming them yield the following equation:

$$\begin{aligned} -2\left(\frac{\pi}{3}\right)^2 J\omega\omega_x - \frac{8}{9}J\omega\omega_x - 2\left(\frac{\pi}{3}\right)^2 J\omega\omega_y\cos\gamma - J\omega\omega_y\cos\gamma = 2\left(\frac{\pi}{3}\right)^2 J\omega\omega_x\cos\gamma + J\omega\omega_x\cos\gamma \\ -2\left(\frac{\pi}{3}\right)^2 J\omega\omega_y\cos\gamma - \frac{8}{9}J\omega\omega_y\cos\gamma \end{aligned} \tag{6}$$

Simplification and transformation of Equation (6) yield the following result:

$$\omega_y = -\left(\frac{2\pi^2+8}{\cos\gamma} + 2\pi^2 + 9\right)\omega_x \tag{7}$$

$\omega_y = -(4\pi^2 + 17)\omega_x$ for the horizontal location of the gyroscope axis ($\gamma = 0$)

where the sign (−) means that the direction of the resistance torque is negative and can be omitted from the following discussions.

Analysis of Equation (6) demonstrates the following algebraic peculiarities. The angular velocities of precessions ω_y and ω_x are variable and depend on the angular location γ of the spinning axis. The left component of Equation (6) contains the torque generated by common inertial forces acting around axis *ox* $T_{inr{\cdot}y} = 2(\pi/3)^2 \times J\omega\omega_y\cos\gamma$, which is equal to the torque generated by centrifugal forces acting around axis *oy* from the right component of Equation (6) $T_{ct{\cdot}y} = 2(\pi/3)^2 \times J\omega\omega_y\cos\gamma$. These torques are self-compensated and can be removed from Equation (5) in the process of

transformation. This peculiarity means the considered internal torques should also be removed from the system of internal kinetic energy generated by rotor's mass elements (Equation (4)). Hence, transformation of Equation (6) yields the following system of equations:

$$J_x\frac{d\omega_x}{dt} = Wgl\cos\gamma + Wl^2\cos\gamma\sin\gamma\omega_y^2 - 2\left(\frac{\pi}{3}\right)^2 J\omega\omega_x - \frac{8}{9}J\omega\omega_x + J\omega\omega_y\cos\gamma$$
$$J_y\frac{d\omega_y}{dt} = 2\left(\frac{\pi}{3}\right)^2 J\omega\omega_x\cos\gamma + J\omega\omega_x\cos\gamma - \frac{8}{9}J\omega\omega_y\cos\gamma \quad (8)$$

$$\omega_y = -\left(\frac{2\pi^2+8}{\cos\gamma} + 2\pi^2 + 9\right)\omega_x$$

The system of Equation (8) enables the gyroscope's angular velocities around axes *ox* and *oy* to be defined. Substituting Equation (7) into the first Equation (8) and their transformation yield the following equation for the gyroscope's motion around axis *ox:*

$$J_x\frac{d\omega_x}{dt} = Wgl\cos\gamma + Wl^2\cos\gamma\sin\gamma\omega_y^2 - 2\left(\frac{\pi}{3}\right)^2 J\omega\omega_x - \frac{8}{9}J\omega\omega_x - \left(\frac{2\pi^2+8}{\cos\gamma} + 2\pi^2 + 9\right)J\omega\omega_x \quad (9)$$

where all components are as specified above.

3. Case study and practical tests

The mathematical model for the motions of the gyroscope suspended from the flexible cord is considered for the horizontal location of the gyroscope spinning axle (cos 0° = 1.0, Figure 1). Substituting the defined gyroscope parameters represented in Tables 2 and 3 as well as in Figure 1 into Equation (9) and their transformation yield the following differential equation:

$$J_x\frac{d\omega_x}{dt} = Wgl\cos\gamma - \left[2\left(\frac{\pi}{3}\right)^2 + \frac{8}{9} + 4\pi^2 + 17\right]J\omega\omega_x \quad (10)$$

$$1.9974649\times10^{-4}\frac{d\omega_x}{dt} = 0.146\times9.81\times0.0325 - \left[2\left(\frac{\pi}{3}\right)^2 + \frac{8}{9} + 4\pi^2 + 17\right]\times0.5726674\times10^{-4}\omega\omega_x$$

Simplification of Equation (10) and its transformation yield the following expression:

$$0.05856228\frac{d\omega_x}{dt} = 13.647215 - \omega\omega_x \quad (11)$$

Separating the variables for the differential Equation (11) yields the following equation:

$$\frac{d\omega_x}{\frac{13.647215}{\omega} - \omega_x} = 17.075837\omega dt \quad (12)$$

Presentation of Equation (12) by the integral form at defined limits yields the following expression:

$$\int_0^{\omega_x}\frac{d\omega_x}{\frac{13.647215}{\omega} - \omega_x} = 17.075837\omega\int_0^t dt \quad (13)$$

The left integral of Equation (13) is tabulated and represented the integral $\int\frac{dx}{a-x} = -\ln x + C$. The right integral is simple. Solving the integrals yields the following expression:

$$-\ln\left(\frac{13.647215}{\omega} - \omega_x\right)\Big|_0^{\omega_x} = 17.075837\omega t\Big|_0^t$$

giving

$$\omega_x = \frac{13.647215}{\omega} \times \left(1 - e^{-17.075837\omega t}\right) \tag{14}$$

It is necessary to underline the one notable result of the analytical approach. For instance, Equation (14) demonstrates that the angular velocity of precession ω_x is variable with time *t*, i.e. with acceleration. Hence, the angular velocity ω_y of the gyroscope around axis *oy* is also variable (third Equation (8)). This equation is validation that the gyroscope is an inertial system. Moreover, the right component of Equation (14) contains the expression $e^{-17.075837\omega t}$ that has a small value of a high order for the angular velocity ω of the spinning rotor, which is about *n* = 10,000 – 30,000 rpm. Hence, this expression can be neglected and the angular velocities of the gyroscope precessions accepted as constant for the common solutions. However, for the low angular velocity of the spinning rotor, the accelerated motion of the gyroscope can be considerable.

Meanwhile, the analysis of Equation (14) demonstrates that the angular velocity of the precession is always decreased with a change of the time *t*, which is a new property of the gyroscope. The angular acceleration of gyroscope precession around axis *ox* is defined by the first derivative of Equation (14) with respect to variable time *t* that has the following expression:

$$\begin{aligned}\varepsilon_x = \frac{d\omega_x}{dt} &= \frac{d\left(\frac{13.647215}{\omega}\right)(1 - e^{-17.075837\omega t})}{dt} = -\frac{13.647215}{\omega} \times (-17.075837\omega) \times e^{-17.075837\omega t} \\ &= 233.037618 \times e^{-17.075837\omega t}\end{aligned} \tag{15}$$

Obviously, the gyroscope's angular acceleration around axis *oy* is represented by the following equation: $\varepsilon_y = (4\pi^2 + 17)\varepsilon_x$.

Equation (15) shows that the gyroscope acceleration is decreasing with time asymptotically to an infinitely small magnitude. The limit of Equation (15) as $t \to \infty$ yields the following result:

$$\lim_{t\to\infty}\left(\frac{233.037618}{e^{17.075837\omega t}}\right) = \frac{233.037618}{e^{17.075837\omega\infty}} \to 0 \tag{16}$$

The conditions of the gyroscope tests are accepted as follows. The rotor speed is *n* = 10,000 rpm or ω = 10,000 (2π/60) rad/s. The drop of the rotor speed due to the action of the friction forces in the gyroscope bearings and by the air viscosity is 67 rev/s. The velocity of the spinning rotor was measured by the Optical Multimeter Tachoprobe Model 2108/LSR Compact Instrument Ltd with a range of measurement of 0–60,000.00 rpm. The time of the gyroscope motions around the axes was measured by a stopwatch model SKU SW01 with a resolution of 1/100 s. The angular measurements of the location for the gyroscope axis were conducted optically by the angular template with an accuracy of $\pm 1.0^0$.

The obtained results of the tests are as follows. The angular velocity of the gyroscope precession around axis *oy* is $\omega_y = 42.188^o$/s and around axis *ox* is $\omega_x = 0.746^o$/s. Moreover, the time spent on one revolution around axis *oy* is $t = 2\pi/\omega_y = 360^o/42.188^o/s = 8.533$ s, and the time spent on the turn of 20° around axis *ox* (±10° around the horizontal location) is $t = 2\pi/\omega_x = 20^o/0.746^o/s = 26.809$ s. The theoretical angular velocity and acceleration of the gyroscope's precession around axes *ox* and *oy* computed by Equations 13, 14 and 7 yield the following result:

$$\begin{aligned}\omega_x &= \frac{13.647215}{\omega} = \frac{13.647215}{2\pi \times 10000/60} = 0.0130387 \quad \text{rad/s} = 0.746^o/\text{s} \\ \varepsilon_x &= \frac{233.037618}{e^{17.075837\omega t}} = \frac{233.037618}{e^{17.075837\times 2\pi\times 10000/60\times 1.0}} = 5.348431 \times 10^{-7708}\text{rad/s}^2\end{aligned} \tag{17}$$

$$\omega_y = (4\pi^2 + 17)\omega_x = (4\pi^2 + 17) \times 0.0130387 = 0.736405 \quad \text{rad/s} = 42.188^o/\text{s}$$
$$\varepsilon_y = (4\pi^2 + 17)\varepsilon_x = (4\pi^2 + 17) \times 5.348431 \times 10^{-7708} \text{rad/s}^2$$

The magnitudes of the angular accelerations around axes *ox* and *oy* are very small of a high order that cannot be measured by high-tech instrumentation. However, the values of the acceleration are very important for the explanation of the gyroscope's angular velocities, which are accepted as constant by researchers. This wrong conclusion results in the wrong statement that the gyroscope manifests non-inertial property.

The experimental and theoretical results of the gyroscope precessions around two axes are presented in Table 4.

Analysis of the tests and theoretical results for the gyroscope time motions around the axes demonstrates that test time is less than theoretical. Explanation of this difference is as follows. The mathematical model of the angular velocities (Equation (17)) does not contain the drop of the angular velocity of the spinning rotor ω, whose decrease leads to increases in the angular velocities of the gyroscope around the axes. Hence, it leads to a decrease in the time of the motions.

The recorded results of the theoretical calculations and practical tests of the gyroscope precessions (Table 4) are well matched in spite of some differences. These differences can be explained by simplifications in the computing of the geometrical parameters for the gyroscope stand and hence in its mechanical properties. Furthermore, the results of the theoretical and practical studies are influenced by the following factors:

- The accuracy level of the computation of the gyroscope's technical data
- The accuracy level of the measurement
- The drop of the spinning rotor velocity and angular precession velocities of the gyroscope
- Variability of the angular velocity of the precession around axes *ox* and *oy*
- Variability of the values of the frictional forces in the supports

All these factors have a definite influence on the computation of gyroscope angular velocities, and in this case the theoretical and practical results will always be different. Generally, the differences in results depend on the quality of the mathematical model and the quality of the practical tests for the process.

The new mathematical model of gyroscope motions enables the explaining of the physics of several gyroscope properties. The small value of the gyroscope accelerations around the axes results in a small value of reactive forces on the supports. Analytically, this is confirmed by the following solution, as the total torque acting around axes *ox* and *oy* on the gyroscope suspended from the flexible cord is defined by the equation $T_{t\cdot i} = J\varepsilon_i$. Then, the reactive force acting on the cord is defined by the following equation:

$$F_i = \frac{T_{t\cdot i}}{l} = \frac{J_i \varepsilon_i}{l} \tag{18}$$

Table 4. Experimental and theoretical results of the gyroscope precession

Gyroscope average parameters	Tests	Theoretical	Difference
Time of precession (one revolution) around axis *oy*	8.2 s	8.533 s	3.90%
Time of precession around axis *ox* on 20° of the turn about horizontal location	25.1 s	26.809 s	6.37%
Angular velocity of precession around axis *ox*	≈1.0°/s	0.746°/s	–

where $T_{t\cdot i}$ is the total torque acting around axis *i*, F_i is the reactive force acting on the cord along the axis, and all other components are as specified above.

Substituting the defined components (Table 2, Figure 2, Equations (17) into Equation (18) and their transformation yield the magnitude of the reactive force of torques acting on the cord along axes *oy* and *ox:*

$$F_y = \frac{J_x \varepsilon_x}{l} = \frac{1.9974649 \times 10^{-4}}{0.0325} \times 5.348431 \times 10^{-7708} = 3.28717021 \times 10^{-7710} N$$
$$F_x = \frac{J_y \varepsilon_y}{l} = \frac{1.9974649 \times 10^{-4}}{0.0325} \times (4\pi^2 + 17) \times 5.348431 \times 10^{-7708} = 1.856541 \times 10^{-7708} N \quad (19)$$

where the reactive force F_y acting on the cord along axes *oy* does not affect an angular location of the gyroscope and has the small value that can be neglected.

The obtained theoretical results validated by practical tests enable the formulating of the following expression: the internal torques acting on the gyroscope do not produce a sensitive reactive force on the supports. The described gyroscope's property is new and should be taken into account for the computation of forces and motions in different gyroscopic mechanisms and devices.

The gyroscope weight *W* gives the reactive force F_W acting along the flexible cord, which is considered with other forces generated by the gyroscope's internal torques for computing the angles of the location of the gyroscope in space relatively to the point of suspension *B* (Figure 4). The centrifugal force acting along horizontal axis *oz* is represented by the sum of the centrifugal forces generated by rotating gyroscope centre-mass around axes *ox* and *oy* as follows:

$$F_{ct\cdot mx} = Wl\omega_x^2 = 0.146 \times 0.0325 \times 0.0130387^2 = 8.066865255 \times 10^{-7}\, N$$
$$F_{ct\cdot my} = Wl\omega_y^2 = 0.146 \times 0.0325 \times 0.7364051^2 = 2.573178081 \times 10^{-3}\, N \quad (20)$$
$$F_z = F_{ct\cdot mx} + F_{ct\cdot my} = 2.573178 \times 10^{-3}\, N$$

The suspended gyroscope represents a movable system, which has a free motion on the horizontal plane *xoz* (Figure 4). The weight of the running gyroscope and the action of internal torques shift the cord along axes *ox, oy* and *oz* relative to the centre axes system Σ*oxyz*. The new location of the end of the gyroscope shaft is o_1 defined by the angles β, φ and ψ, and by the linear distance *a* and *b*. The angle ψ is calculated by the formula: $\sin\psi = a/d$.

The internal torques acting around axis *oy* turn the gyroscope through an angle β in a counterclockwise direction relative to its centre of gravity *A*. The end of the flexible cord *o* is shifted on the distance *b* on the plane *xoy*. However, the angle β is restricted by the balancing of the force F_x of the torques and by the force of the gyroscope's weight component F_1 acting along axis *ox*. The centrifugal force F_z acting along axis *oz* turns the gyroscope through an angle ψ around the point of suspension *B* at the plane *zoy*. The end of the flexible cord *o* is shifted on the distance *a*. However, the angle ψ is restricted by the balancing of the force F_z of the torques and by the force of the gyroscope's weight component F_2 acting along axis *oz*.

Figure 4 enables the value of the reactive forces to be defined by the following formulas: $F_x = T_{ty}/l$, where T_{ty} is the total torque acting around the cord (axis *oy*); $F_2 = Wl\omega_y^2$, where ω_y is the angular velocity of precession around axis *oy* and other parameters are as specified above. In this circumstance, the end of the cord *o* turns around the point of suspension *B* on the angles φ and ψ. Figure 4 enables the angles φ, β and ψ to be defined by the following formulas: $\sin\varphi = F_1/F_W$, where F_W is the force of gyroscope weight; $\sin\beta = b/l$, where $b = d\sin\varphi$; *d* is the length of the cord; $\sin\psi = F_2/F_W$ and other parameters are as specified above. Thus, the balance of the action of the forces ($F_1 = F_x$) and ($F_2 = F_z$) enables the angular location φ and ψ about the vertical of the cord to be defined by the following solutions:

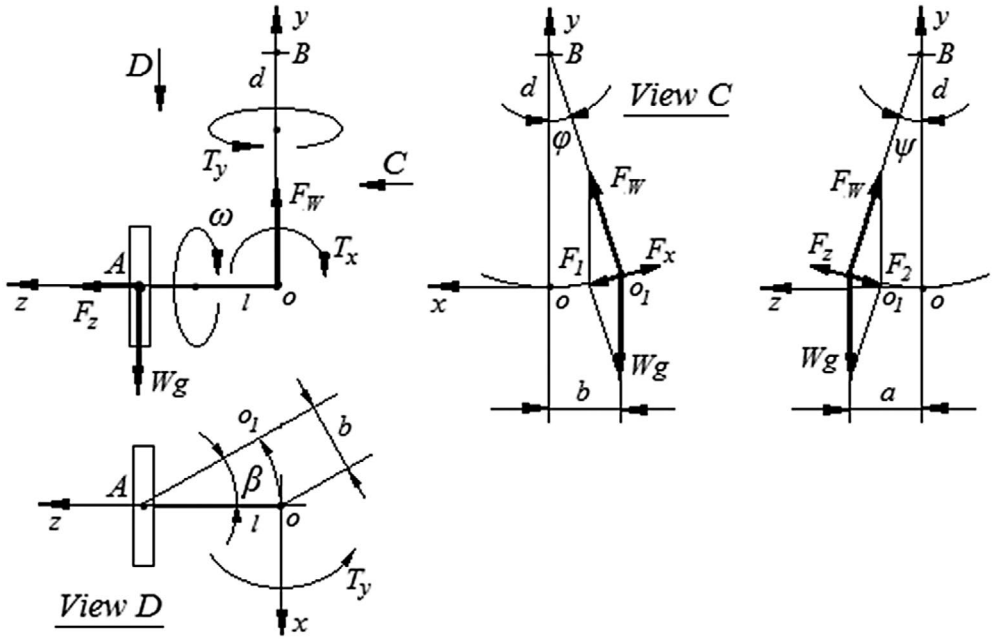

Figure 4. Location of the gyroscope suspended from the flexible cord.

$$\sin\phi = \frac{F_1}{F_W} = \frac{1.856541 \times 10^{-7708}}{0.146 \times 9.81} = 1.296232 \times 10^{-7708}$$
$$\sin\psi = \frac{F_z}{F_W} = \frac{2.573178 \times 10^{-3}}{0.146 \times 9.81} = 0.00179658. \quad (21)$$

giving $\varphi \approx 0^{\circ}$ and $\psi = 0.102^{\circ}$ Then, the distance $b = \varphi d = 0 \times 250 \approx 0$ mm, which gives the value of the angle $\sin\beta = b/l = 0/32.5$, hence $\beta = 0^{\circ}$. The distance $a = \psi d = (0.102^{\circ} \times \pi/180^{\circ}) \times 250 = 0.449$ mm. The end of the cord is shifted on a very small distance at the plane *xoz* that can be neglected. Apart from that, the vertical location of the cord with the suspended gyroscope is validated by the tests and demonstrate no appreciable decline of the cord from the vertical.

Practical tests of the suspended gyroscope with a high angular velocity of the rotor demonstrate that such a system does not manifest the motions of a swinging pendulum. This is because the action of the internal torques presents the gyroscope as an over-damped or critically damped non-oscillating system. However, the low angular velocity of the rotor leads to the gyroscope oscillation.

4. Results and discussion

The analytical study of forces acting on the gyroscope suspended from the flexible cord formulated the mathematical model of its motions around two axes. These motions resulted from the acting of the centrifugal, common inertial, and Coriolis forces and the change in the angular momentum of the spinning rotor. For instance, acting forces generated the resistance and precession torques, which produce the different angular velocities of the gyroscope around the two axes. The angular velocities are variable, but their changes are insignificantly small and can be neglected for practical application. It is found that the acting torques do not generate the sensitive reactive force on the support that the new gyroscope property was proven analytically and practically, which should be taken into account for engineering computing. In addition, the mathematical models for the gyroscope motions suspended from the flexible cord, as well as the action of the external and internal torques, are validated by practical tests. The results of the gyroscope time motions around two axes and acting forces computed by mathematical models are well matched with the practical tests. Thus, the obtained results are the validations of the correctness of the new analytical approach.

5. Conclusion

The gyroscope theory in classical mechanics is one of the most complex and intricate in terms of analytical solutions. The known mathematical models for the gyroscope theory are mainly based on the action of the external torque applied and the change in the angular momentum of the spinning rotor. This approach involves many assumptions and simplifications of the unexplainable motions of gyroscopic devices. However, new studies demonstrate that the torques generated by the centrifugal, common inertial and Coriolis forces of the mass elements of the spinning rotor play a critical role along with the change in the angular momentum. The action of each force is formulated by the mathematical model for the gyroscope motions suspended from the flexible cord that was most unsolvable. Other than that, the new analytical approach for the gyroscope effects clearly describes the known properties and reveals a new one. The experimental tests of the motions and forces acting on the gyroscope are suspended from a flexible cord, which matches well the mathematical model. Thus, the new analytical approach represents the gyroscope properties in a new light and constitutes new challenges for future studies of gyroscopic devices.

Nomenclature

b	shift distance of the end of a gyroscope shaft relatively axis *oy*
d	length of a flexible cord
g	gravity acceleration
e	base of natural logarithm
F_i	reactive force of a support along axis *i*
$F_{ct{\cdot}my}$	centrifugal force of rotation gyroscope centre-mass around axis *oy*
W	weight of a gyroscope
i	index for axis *ox* or *oy*
J	mass moment of inertia of a rotor's disc
J_i	mass moment of inertia of a gyroscope around axis *i*
m	mass of a rotor's disc
l	distance between a gyroscope centre mass and a cord
R	external radius of a rotor
T	load torque
$T_{am{\cdot}i}$	torque generated by a change in an angular momentum acting around axis *i*
T_{ct}, $T_{cr{\cdot}i}$, $T_{in{\cdot}i}$	torque generated by centrifugal, Coriolis and common inertial forces, respectively, and acting around axis *i*
$T_{ct{\cdot}my}$	torque generated by centrifugal force of a rotating gyroscope centre mass and acting around axis *oy*
T_p	precession torque acting around axis
T_r	resistance torque acting around axis
$T_{t{\cdot}i}$	total torque acting around axis
iT	time
B	angle of gyroscope turn on a plane *xoz*
φ, ψ	angle of gyroscope turn around of a cord suspension along axis *ox* and *oz*, respectively
ε_i	angular acceleration of a gyroscope around axis *i*
γ	angle of inclination of a rotor's axle
ω	angular velocity of a rotor
ω_i	angular velocity of precession around axis *i*

Funding
The author received no direct funding for this research.

Author details
Ryspek Usubamatov[1]
E-mail: ryspek0701@yahoo.com
[1] Mechanical, Manufacturing and Industrial Engineering, International University of Kyrgyzstan, 255 Chui Avenue, Bishkek, Kyrgyz Republic.

Citation information
Cite this article as: A mathematical model for motions of gyroscope suspended from flexible cord, Ryspek Usubamatov, *Cogent Engineering* (2016), 3: 1245901.

Cover image
Source: Author.

References

Aardema, M. D. (2005). *Analytical dynamics. Theory and application*. New York, NY: Academic/Plenum Publishers.

Braun, R. D., Putnam, Z. R., Steinfeldt, B. A., Grant, M. J., & Barton, G. (2013). *Advances in inertial guidance technology for aerospace systems (AIAA 2013-5123)*, AIAA Guidance, Navigation, and Control (GNC) Conference. doi:10.2514/6.2013-5123

Cordeiro, F. J. B. (2015). *The gyroscope*. Las Vegas, NV: Create space.

Crassidis, J. L., & Markley, F. L. (2016). Three-axis attitude estimation using rate-integrating gyroscopes. *Journal of Guidance, Control, and Dynamics*, 1–14. doi:10.2514/1.G000336

Doupe, C., & Swenson, E. D. (2016). Optimal attitude control of agile spacecraft using combined reaction wheel and control moment gyroscope arrays, (AIAA 2016-0675). *AIAA Modeling and Simulation Technologies Conference*. doi:10.2514/6.2016-0675

Greenhill, G. (2015). *Report on gyroscopic theory*. Fallbrook, CA: Relnk Books.

Gregory, R. D. (2006). *Classical mechanics*. New York, NY: Cambridge University Press. http://dx.doi.org/10.1017/CBO9780511803789

Inampudi, R., & Gordeuk, J. (2016). Simulation of an electromechanical spin motor system of a control moment gyroscope. *AIAA Guidance, Navigation, and Control Conference*, San Diego, CA. doi:10.2514/6.2016-0091

Jonsson, R. M. (2007). Gyroscope precession in special and general relativity from basic principles. *American Journal of Physics, 75*, 463. doi:10.1119/1.2719202

Liang, W. C., & Lee, S. C. Vorticity, gyroscopic precession, and spin-curvature force. *Physical Review D, 87*, 044024. Retrieved February 11, 2013, from http://dx.doi.org/10.1103/PhysRevD.87.044024

Neil, B. (2014). *Gyroscope*. Cambridge, Massachusetts: The Charles Stark Draper Laboratory. doi:10.1036/1097-8542.304100

Scarborough, J. B. (2014). *The gyroscope theory and applications*. London: Nabu Press.

Stevenson, D., & Schaub, H. (2012). Nonlinear control analysis of a double-gimbal variable-speed control moment gyroscope. *Journal of Guidance, Control, and Dynamics, 35*, 787–793. doi:10.2514/1.56104

Usubamatov, R. (2015, May 15). Mathematical model for gyroscope effects. *AIP Conference Proceedings American Institute of Physics*. doi:10.1063/1.4915651

Usubamatov, R. (2016). Gyroscope internal kinetic energy and properies. *International Journal of Advancements in Mechanical and Aeronautical Engineering, 3*, 16–20.

Usubamatov, R. (2014). Properties of gyroscope motion about one axis. *International Journal of Advancements in Mechanical and Aeronautical Engineering, 2*, 39–44. ISSN:I2372-4153.

Weinberg, H. (2011). *Gyro mechanical performance: the most important parameter* (Technical Article MS-2158) (pp. 1–5). Norwood, MA: Analog Devices.

Zhang, N., Ren, Y. F., & Li, S. K. (2012). Research on testing method of dynamic characteristic for MEMS-gyroscope. *Advanced Materials Research, 346*, 515–520.